Supersonic Flutter of Aeroelastically Tailored Oblique Wings

Terrence A. Weisshaar* and Jonathan D. Bohlmann†
Purdue University, West Lafayette, Indiana

Renewed interest in oblique wing aircraft has created curiosity about the possible use of aeroelastic tailoring to enhance its aeroelastic stability. This paper examines the flutter characteristics of an idealized, advanced composite, oblique wing configuration operating at supersonic speeds. The theoretical model consists of a uniform property wing with beamlike flexural and torsional flexibility as well as bend-twist deformation cross-coupling. The wing is free to roll unrestrained about a streamwise roll axis. Quasisteady, linearized, supersonic aerodynamic theory is used to describe the deformation-dependent aerodynamic forces. The effects of characteristic inertial, aerodynamic, and structural parameters on flutter behavior are surveyed. Among these parameters are the following: wing aspect ratio; mass ratio; Mach number; fundamental bending-torsion frequency ratio; bend-twist deformation coupling; wing sweep angle; and the wing-to-fuselage roll mass moment of inertia ratio. It is shown that when tailoring is used to increase the stability of a body-freedom mode, the result is a reduction of stability of other high-frequency aeroelastic modes. This tradeoff characteristic is similar to that observed for conventional wings and indicates that excessive wing stiffness cross-coupling is undesirable as a passive measure to control flutter.

Introduction

AFTER an absence of nearly 10 years, the oblique wing concept of the type sketched in Fig. 1 is again receiving serious consideration.[1] During this 10-year period, significant technological advancements have occurred in a number of areas important to oblique wing development. These advances, coupled together with new needs and opportunities, are such that the oblique wing concept deserves serious consideration as a contender for future civil and military missions. However, design features unique to the oblique wing still remain to be considered carefully. Chief among these features are asymmetrical aeroelastic effects introduced by the unconventional wing orientation.

Early oblique wing aeroelastic stability studies established the necessity of including aircraft roll freedom in aeroelastic analysis or wind-tunnel testing.[2-6] Roll freedom allows the classical forward-swept-wing aeroelastic divergence mode to be replaced by a low-frequency, oscillatory "body-freedom flutter" instability that occurs at a higher flight dynamic pressure than does wing divergence. The inclusion of fuselage pitch and plunge freedoms leads to an additional increase in the low-frequency instability speed, but their inclusion is much less important than roll freedom. The low-frequency flutter instability is "divergence driven"; a stiffness change that increases the theoretical divergence speed usually will be found to increase the oblique wing body-freedom flutter speed.

The purpose of the present study is to examine the importance and the effect of certain design parameters on aeroelastic stability features of oblique winged aircraft operating at supersonic speeds. The first portion of the study is restricted to orthotropic wing structures to assess the importance of several conventional parameters to oblique wing supersonic flutter and also to underscore the presence of a sizable number of design parameter combinations. Finally, the study focuses on the inclusion of a bounded laminate stiffness design parameter that defines and permits bend-twist wing deformation coupling. The effect of this coupling parameter on aeroelastic stability is illustrated and its influence compared to the influence of geometrical wing sweep on oblique wing flutter. Let us now turn to a discussion of the analytical model used for this study.

Aeroelastic Model

The theoretical model developed for this study provides a simple, effective method for displaying the potential effects of laminate tailoring on oblique wing aeroelastic stability. The structural idealization itself has been used in previous oblique wing studies[4] (but without stiffness cross-coupling) and has revealed accurately oblique wing flutter trends in the low-speed flow region. Figure 2 shows the planform geometry of the idealization. As indicated, taper was not considered as a study parameter. Although the wing is swept at an angle Λ with respect to the flow, note that the wingtips are not parallel to the flow except when Λ is zero.

Although the complex built-up structure of an actual aircraft wing is composed of numerous internal members and a cover skin, for this idealization the combined effect of these structural elements is lumped into three essential stiffness parameters. Figure 3 shows the cross section of a beamlike element to illustrate the deformations w and θ and internal resultant moments M and T. The y axis in Fig. 3 is the reference axis (RA), which is also shown in Fig. 2. Conventional engineering beam models choose the RA to be the shear center, the position where a shear force can be applied without causing twist at that section. As a result, bending and twisting deformation of an orthotropic beam are uncoupled when static equilibrium equations are written with respect to this axis.

If the beam is anisotropic, then at any cross section the relationship between the internal moment resultants (bending moment M and torque T), and the beam curvature $\partial^2 w/\partial y^2$, and

Presented as Paper 87-0734 at the AIAA/ASME/AHS/ASEE 28th Structures, Structural Dynamics and Material Conference, Monterey, CA, April 6-8, 1987; received June 9, 1987; revision received July 6, 1988. Copyright © 1987 American Institute of Aeronautics and Astronautics, Inc. All rights reserved.

*Professor, School of Aeronautics and Astronautics. Associate Fellow AIAA.

†Graduate Research Assistant; currently, Engineer, General Dynamics Corporation, Ft. Worth, TX. Member AIAA.

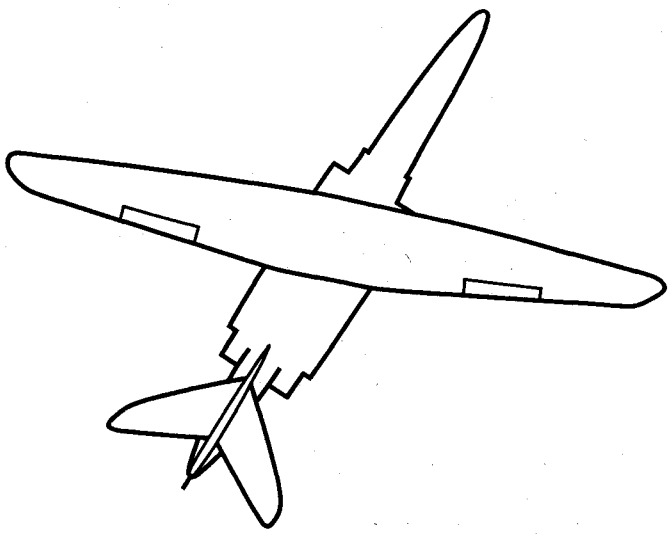

Fig. 1 Hypothetical oblique wing aircraft configuration.

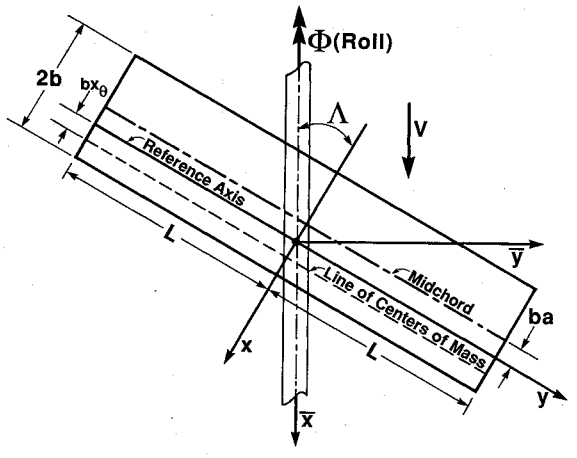

Fig. 2 Analytical model planform geometry, showing definitions of axis systems, the reference axis, dimensions and center-of-mass position.

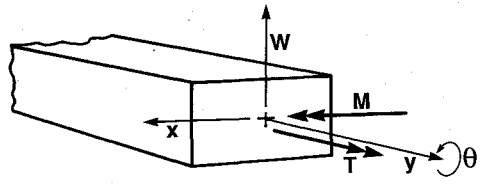

Fig. 3 Anisotropic beam cross-section showing internal resultant moments and deformation sign convention.

twist rate $\partial\theta/\partial y$, may be expressed as

$$\begin{Bmatrix} M \\ T \end{Bmatrix} = \begin{bmatrix} EI & -K \\ -K & GJ \end{bmatrix} \begin{Bmatrix} w'' \\ \theta' \end{Bmatrix} \tag{1}$$

The primes refer to differentiation with respect to y. Three anisotropic beam stiffness parameters appear in Eq. (1): EI, a bending stiffness parameter; GJ, a torsional stiffness parameter; and K, a bend-twist coupling parameter. The parameter K creates the effect called "stiffness cross-coupling" and depends on the RA location and the laminate details, as well as internal structural member arrangements; K may be positive, negative, or zero. For an orthotropic beam, the RA is chosen so that $K=0$.

The relationship in Eq. (1) can be inverted to obtain a flexibility relation, written as[7]

$$\begin{Bmatrix} w'' \\ \theta' \end{Bmatrix} = \frac{1}{1-kg} \begin{bmatrix} 1/EI & g/EI \\ g/EI & 1/GJ \end{bmatrix} \begin{Bmatrix} M \\ T \end{Bmatrix} \tag{2}$$

where $g=K/GJ$ and $k=K/EI$.

Strain energy considerations require the value of kg (a nondimensional product) to lie between zero and unity. This product may be expressed conveniently in terms of a nondimensional stiffness cross-coupling parameter Ψ, defined by the relationship

$$\Psi^2 = K^2/EI\,GJ < 1 \tag{3}$$

As a result, Ψ is bounded as follows:

$$-1 < \Psi < 1 \tag{4}$$

Because of the definitions of w, θ, M, and T in Eqs. (1) and (2), negative values of K are associated with configurations in which upward bending ($+w$ and $+w''$) is accompanied by nose-down twist ($-\theta$). How one actually achieves this deformation or stiffness cross-coupling, as represented by K, is a matter of design ingenuity. Design strategies for such coupling range from: the development of flexible hinge-line orientation for folding wings and all-movable tails; off-axis spar orientations; and tailored anisotropic skins for lifting surfaces. Of all the ideas proposed to date, the most promising seems to be that of anisotropic, unbalanced (but midplane symmetric) laminated wing skin surfaces.

Figure 4 provides an example of the type of deformation coupling that will result from directional ply orientation of a single-ply composite plate. It is seen from Fig. 4a that, when the plies are oriented along the spanwise direction, an upward aerodynamic load causes bending deformation that, viewed from the side, results in a decrease in the streamwise angle of attack. As indicated in Fig. 4b, the off-axis rotation of plies will cause bend-twist deformation cross-coupling (more commonly called stiffness cross-coupling) that leads to the opposite situation. The first situation is referred to as washout behavior, whereas the second is called wash-in behavior.

Numerous external and internal structural details, particularly laminate geometry, determine and control the values of EI, GJ, and K. A change in one such detail, e.g., skin orientation, will cause simultaneous changes in all three stiffness parameters. As a result, the credit for a change in aeroelastic performance (e.g., an increase in flutter speed) caused by rotation of a certain laminate ply may be difficult to attribute to EI, GJ, or K, because all three change. The focus of this study will be solely on the influence of stiffness cross-coupling K; as a result, EI and GJ are held fixed. In practice, this would require a redesign of the cross-sectional structural geometry each time K is changed. Although this might be viewed as a limitation, the purpose of the present study is to assess the effectiveness of oblique wing tailoring using bend-twist deformation coupling, but not to design an actual oblique wing aircraft.

Equation (1) may be used to develop the strain energy stored in an advanced composite beam/wing. This strain energy U, is

$$U = \frac{1}{2}\int_0^L \left\{ EI\left(\frac{\partial^2 w}{\partial y^2}\right)^2 - 2K\left(\frac{\partial^2 w}{\partial y^2}\right)\left(\frac{\partial\theta}{\partial y}\right) + GJ\left(\frac{\partial\theta}{\partial y}\right)^2 \right\} dy \tag{5}$$

The expression in Eq. (5), when used with assumed deflection functions for $w(y,t)$ and $\theta(y,t)$, is used to construct the wing structural stiffness matrix used for this study.

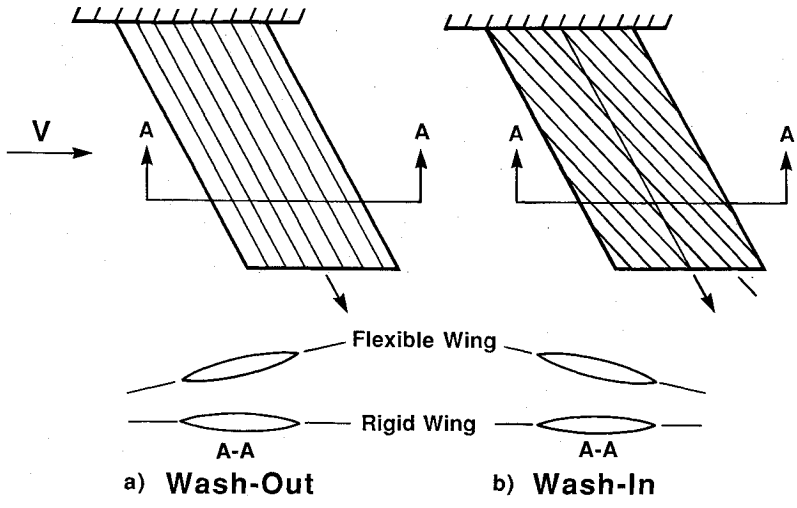

Fig. 4 Effects of wing geometry and ply orientation on streamwise angle of attack due to bending deformation.

A plate model also might be used to model the wing structural deformation. In this case, *EI*, *GJ*, and *K* are computed from a knowledge of equivalent plate constants. Note that the expression in Eq. (5) does not include one potentially important plate stiffness term, a term that is found to be proportional to $(\partial^2\theta/\partial y^2)^2$. The origin of this stiffness term is traceable to the requirement that a cantilever plate edge not only remain untwisted, but it must remain undeflected along the root support. Because of its one-dimensional character, a beam model cannot enforce this latter condition. A chordwise structural stiffness term S_0 multiplies this torsional curvature term. For moderately high-aspect-ratio metallic structures whose ratio of shear modulus G to Young's modulus E is small, this warping term is of little consequence. However, for composite materials whose ratio of effective moduli is rather large, the effect of this additional term may be significant, even when the structural aspect ratio is large.[8] However, for this study, the possibility of increased torsional restraint due to this term is not included.

Aerodynamic Forces

The deformation-dependent aerodynamic forces are modeled using a quasisteady, second-order piston theory. The merits of this theory are discussed by Morgan et al.[9] The basic assumptions of piston theory are that the aerodynamic profile is slender and that the Mach number is high ($M^2 \gg 1$). A modification of ordinary piston theory, due to Van Dyke,[10] is used for the present aeroelastic model. Van Dyke's theory presumes that the flow is quasisteady, but, unlike piston theory, it contains no restriction that the Mach number is large in comparison to unity.

In terms of the planform coordinates defined in Fig. 2, the linearized expression for the pressure differential Δp on the wing is, from piston theory,

$$\Delta p(x,t) = -2\rho_\infty a_\infty \left[V\frac{\partial w}{\partial \bar{x}} + \frac{\partial w}{\partial t} \right] \tag{6}$$

where a_∞ is the speed of sound and ρ_∞ the air density. Since the streamwise coordinate $\bar{x}$ (shown in Fig. 2) is a function of spanwise coordinates x and y, the derivative $\partial w/\partial \bar{x}$ is written as

$$\frac{\partial w}{\partial \bar{x}} = \frac{\partial w}{\partial x}\cos\Lambda + \frac{\partial w}{\partial y}\sin\Lambda \tag{7}$$

The out-of-plane displacement of the wing shown in Fig. 2 is decomposed into two parts—that due to wing flexibility and that due to rigid-body rolling motion. The displacement of the wing surface $w(x,y,t)$, is now written as

$$w(x,y,t) = w_F(y,t) - x\theta(y,t) + \Phi\cos\Lambda(y - x\tan\Lambda) \tag{8}$$

Equation (8) does not allow camber bending (bending displacement or curvature along the x axis). The bending displacement $w_F(y,t)$ is measured with respect to the fuselage root along the reference axis. Using Eqs. (7) and (8), the pressure differential can be expressed in terms of spanwise and chordwise derivatives, as follows:

$$\Delta p(x,y,t) = -2\rho_\infty a_\infty V\cos\Lambda\{w_F'\tan\Lambda - \theta - x\theta'\tan\Lambda + (1/V\cos\Lambda)(\dot{w}_F + \dot{\Phi}\cos\Lambda - x\dot{\theta})\} \tag{9}$$

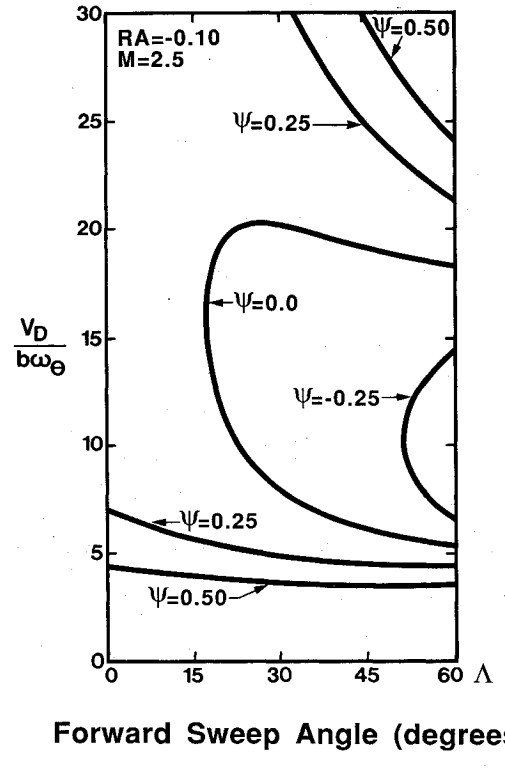

Fig. 5 Effect of stiffness cross-coupling and wing forward-sweep angle on sweptforward wing divergence speed. Reference axis/shear center position is located 0.10 semichord ahead of the midchord line; $M = 2.5$.

In Eq. (9), the primes refer to partial differention with respect to y, whereas the overdots represent partial differentiation with respect to time. The Principle of Virtual Work and the Rayleigh-Ritz method are then used to define the generalized forces Q_i for the system in terms of Δp and chosen assumed displacements of the flexible wing surface.

Kinetic Energy

When Eq. (8) is differentiated with respect to time t, and then integrated into the chordwise direction, the kinetic energy of the wing T_w can be written in the following integral form:

$$T_w = \frac{1}{2}\int_{-L}^{L} \{m\dot{w}_F^2 + (\dot{\Phi}\cos\Lambda)^2 (my^2 - 2Sy\tan\Lambda + I_\theta \tan^2\Lambda) + I_\theta\dot{\theta}^2 - 2\dot{w}_F\dot{\theta}S + 2\dot{w}_F\dot{\Phi}\cos\Lambda(my - S\tan\Lambda) - 2\dot{\theta}\dot{\Phi}\cos\Lambda(Sy - I_\theta\tan\Lambda)\}\,dy \tag{10}$$

Integration into the chordwise direction defines inertia terms, the symbols S, I_θ, and m, written as follows:

$$m = \int \rho\, dx \tag{11a}$$

$$S = \int \rho x\, dx = mbx_\theta \tag{11b}$$

$$I_\theta = \int \rho x^2\, dx = mb^2 r_\theta^2 \tag{11c}$$

Added to Eq. (10) is the kinetic energy due to fuselage rotation, expressed as T_f,

$$T_f = \tfrac{1}{2} I_f \dot{\Phi}^2 \tag{12}$$

These equations of motion for this model describe the transient motion of the system that results when it is slightly perturbed from an initial, deformed, and static equilibrium position.

Equations of Motion

The choice of polynomials as assumed displacement functions, their substitution into Eqs. (5), (9), and (10), and subsequent integration make it possible to use Lagrange's equations to produce a set of linear algebraic equations of motion. Nondimensionalization provides a set of equations of motion having the following matrix form:

$$[M_{ij}]\{\ddot{\xi}\} + [B_{ij}]\{\dot{\xi}\} + [K_s]\{\xi\} + (V/b\omega_\theta)^2[1/(M^2-1)][\bar{K}]\{\xi\} = \{0\} \tag{13}$$

The vector $\{\xi\}$ is constructed as follows:

$$\{\xi\} = \begin{Bmatrix} w_R/L \\ \theta_R \\ w_L/L \\ \theta_L \\ \Phi\cos\Lambda \end{Bmatrix} \tag{14}$$

The symbols w_R and w_L represent wingtip bending deformation, whereas θ_R and θ_L are the wingtip twist angles. Combining the structural stiffness matrix $[K_s]$ and the aerodynamic stiffness matrix into a single matrix $[K]$, Eq. (13) is rewritten as

$$[M]\{\ddot{\xi}\} + [B]\{\dot{\xi}\} + [K]\{\xi\} = \{0\} \tag{15}$$

Note that $[M]$, $[B]$, and $[K]$ are matrices of real numbers, while $\{\xi\}$ represents a vector consisting of the five generalized displacements. The $[B]$ matrix is a function of aerodynamic parameters such as Mach number. The lengthy expressions for the elements of these matrices are presented in Ref. 11.

The equations of motion are written in state-space form as follows:

$$\{\dot{z}\} = [A]\{z\} \tag{16}$$

The 10 elements of the state vector $\{z\}$ represent the five generalized displacements and their corresponding time derivatives. This vector is written as

$$\{z\} = \{\xi/\dot{\xi}\} \tag{17}$$

The matrix $[A]$ contains the equation of motion together with the identity defining the state vector $\{z\}$. Using the matrices defined in Eq. (15), $[A]$ is written as

$$[A] = \begin{bmatrix} 0 & I \\ -M^{-1}K & -M^{-1}B \end{bmatrix} \tag{18}$$

The Laplace transform of Eq. (16) provides an eigenvalue problem. The eigenvalues of the Laplace transform of $[A]$ are written as

$$s = (\sigma/\omega_\theta) + (j\omega/\omega_\theta), \qquad j = \sqrt{-1} \tag{19}$$

The parameter ω_θ is a reference torsional stiffness parameter used for parameter nondimensionalization. The real part of s may be interpreted as the system damping, whereas the imaginary part corresponds to the oscillatory part of the transient response of the disturbed system. As a result, the aeroelastic stability criterion becomes that of examining the sign of σ/ω_θ. If σ/ω_θ is greater than zero, the system is unstable.

Nondimensional Parameters Affecting Flutter Speed

The reference frequency ω_θ represents the natural frequency of a uniform cantilever beam of length L when the beam is excited in an uncoupled torsion mode. The reference bending frequency ω_B is a similar parameter used to represent the uncoupled cantilever fundamental bending frequency. These reference parameters were used to replace the stiffness parameters GJ and EI, respectively. Both modes would occur ar zero airspeed only when the wing static imbalance x_θ and stiffness parameter K are zero. As a result, there is no simple relationship between K and ω_B and ω_θ. However, a relationship between K, Ψ, ω_θ, and ω_B can be developed by integrating the Rayleigh-Ritz shape functions. Integration provides the following relationship[11]:

$$K = \Psi\sqrt{(13/486)}mbr_\theta L^3\omega_B\omega_\theta \tag{20}$$

The factor under the square root sign is unique to the shape functions used for this study. As a result of Eq. (20), the parameter K can be replaced by reference quantities.

Several other important parameters appear in the matrices that define the equations of motion. A term $\bar{AR} = L/b$ defines the aspect ratio of the unswept wing. Note from Fig. 2 that the wingspan, tip to tip, is $2L$ and that $b = c/2$. A nondimensional static unbalance term x_θ, shown in Fig. 2, represents the location of the sectional centers of mass, measured positive aft of the reference axis in units of semichords. Negative values of x_θ imply that the line of centers of mass is forward (toward the leading edge) of the RA. Similarly, the nondimensional parameter a shown in Fig. 2 locates the RA position in units of b, with respect to the midchord position. A negative value of a indicates that the reference axis is forward of the midchord.

The parameter r_θ is a nondimensional radius of gyration of the chordwise section, measured about the RA. A mass ratio parameter μ, defined as $m/\pi\rho b^2$, describes the relative density ratio of a wing section to the air density, whereas the Mach number M defines the speed regime. Finally, the frequency ratio ω_B/ω_θ is a measure of the relative stiffnesses in bending and torsion at zero airspeed when x_θ and K are zero.

Let us now turn to the examination of the results of several analyses whose purpose was to identify the influence of parameters, particularly stiffness cross-coupling, on aeroelastic stability. The first task will be to examine the influence of the cross-coupling parameter Ψ on the divergence of a symmetrical, supersonic, forward-swept wing fixed at the root ($\Phi=0$).

Oblique Wing Aeroelastic Stability—Roll Freedom Excluded

The eigenvalues s of the matrix $[A]$ in Eq. (18) are velocity dependent. The stability analysis begins by fixing M and selecting a range of airspeeds (in this case, nondimensional airspeed $V/b\omega_\theta$); at a given airspeed, values of s are then determined. Wing divergence is a special instability that occurs when, at a certain airspeed, one of these eigenvalues migrates from the left half-plane to the right half-plane of a root-locus plot by passing through the origin. At wing divergence, an eigenvalue is located at the origin of this graphical display ($s=0$). If the airspeed is increased slightly, the real part of the eigenvalue becomes positive, while the imaginary part remains zero; motion is of the form e^{st} and clearly unstable.

Because of this special mathematical feature, i.e., $s=0$, divergence is often referred to as a "static" instability. The term static is used because inertia and damping effects are not present in Eq. (13) when $s=0$. As a result, the dynamic instability problem may be recast in the following form, with a dynamic pressure parameter λ as the eigenvalue:

$$\{[K_s]-\lambda^2[K_A]\}\{z\}=\{0\} \tag{21}$$

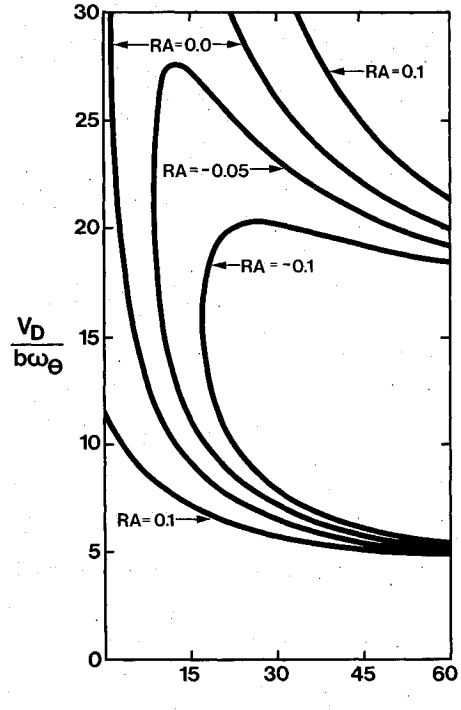

Fig. 6 Effect of reference axis/shear center position on the divergence speed of an orthotropic sweptforward wing. The divergence velocity parameter is plotted against forward-sweep angle. No stiffness cross-coupling is present. RA values indicate magnitude of a used in the analysis.

Equation (21) contains both the structural stiffness matrix $[K_s]$ and the aerodynamic stiffness matrix $[K_A]$. This latter matrix is multiplied by the eigenvalue parameter λ^2, defined as

$$\lambda^2=\frac{M^2}{\sqrt{M^2-1}}\left(\frac{a_\infty}{b\omega_\theta}\right)^2\left(\frac{1}{\pi\mu}\right) \tag{22}$$

The behavior of this eigenvalue λ^2, as a function of stiffness cross-coupling, will be examined. The combination $(b\omega_\theta/a_\infty)\sqrt{\mu}$ occurring in Eq. (22) is referred to as the "stiffness-altitude parameter" and is sometimes denoted as β in aeroelastic literature. However, because the present interest focuses on isolating the effects of the nondimensional parameter Ψ on divergence, the Mach number and the mass ratio μ (but not the speed of sound) will be fixed in the studies to follow. In this case, λ is proportional to $(V/b\omega_\theta)$, written as $\bar{V}$.

First, consider a clamped sweptforward wing with the following physical parameters:

$$\overline{AR}=12, \quad x_\theta=-0.1, \quad (\omega_B/\omega_\theta)=0.2$$

$$r_\theta=0.4, \quad \mu=50, \quad a=-0.10, \quad M=2.5$$

[Note that, although some of these parameters are inertial, when the determinant of Eq. (21) is expanded and dimensional expressions are inserted, only stiffness terms will remain to define the divergence speed.]

Figure 5 shows the results of a divergence analysis of the isolated, clamped forward-swept wing portion of an oblique wing with a variable-sweep angle. Consider first the case labeled $\Psi=0$. Figure 5 indicates that, without deformation cross-coupling, the wing will not encounter divergence instability unless it is swept forward about 17 deg. If the wing is swept forward beyond 17 deg, the airspeed at which it will diverge declines rapidly with sweep. Note that there is both a lower portion and an upper portion to the stability boundary in Fig. 5. At a fixed forward-swept angle, say 30 deg, increasing the airspeed will lead to divergence (contact with the lower boundary). Further increases in airspeed will lead to contact with the upper boundary. At this point, an airspeed increase will lead to a restabilization of the unstable wing.

Consider now the curve labeled $\Psi=-0.25$, corresponding to moderate, negative (bend-up/twist-down) cross-coupling to create washout. As indicated in Fig. 5, negative cross-coupling is stabilizing and tends to displace the $\Psi=0$ static stability boundary to the right. As a result, with $\Psi=-0.25$, no static instability is expected unless forward-swept angles are in excess of 45 deg.

The addition of wash-in in the form of positive (bend-up/twist-up) cross-coupling is seen to be destabilizing. If $\Psi=-0.25$, the wing must be swept aft (the region $\Lambda<0$ in Fig. 5) to create sufficient washout to preclude divergence. Note that large positive cross-coupling, $\Psi=0.50$, is very destabilizing.

Let us now examine the effect of the chordwise shear center position with respect to the midchord on divergence of a wing without stiffness cross-coupling. In this case, the RA is the line of shear centers. The shear center position when $\Psi=0$ is determined by the chordwise thickness distribution of laminate plies and the location of the wing box within the wing cross section. To illustrate the effects of shear center position, consider Fig. 6. This figure displays the nondimensional divergence speed parameter plotted against the forward-swept angle for the same wing described in Fig. 5, but with zero deformation cross-coupling. Note that the curve labeled RA $=-0.1$ (the value of a is -0.1) in Fig. 6 corresponds to that labeled $\Psi=0$ in Fig. 5.

Consider first an RA/shear center position at the midchord ($a=0$). The chordwise position of the aerodynamic center is

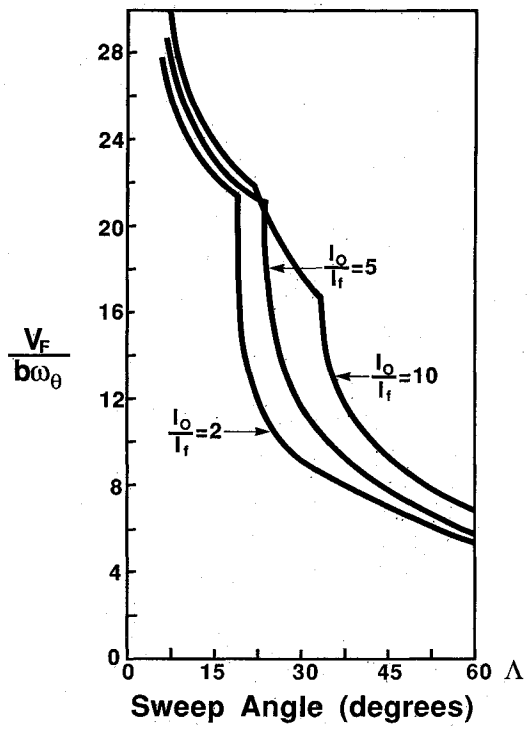

Fig. 7 Effect of the roll-mass-ratio parameter I_0/I_f on flutter speed of the baseline orthotropic oblique wing with freedom to roll. Stiffness cross-coupling is excluded; $M=1$.

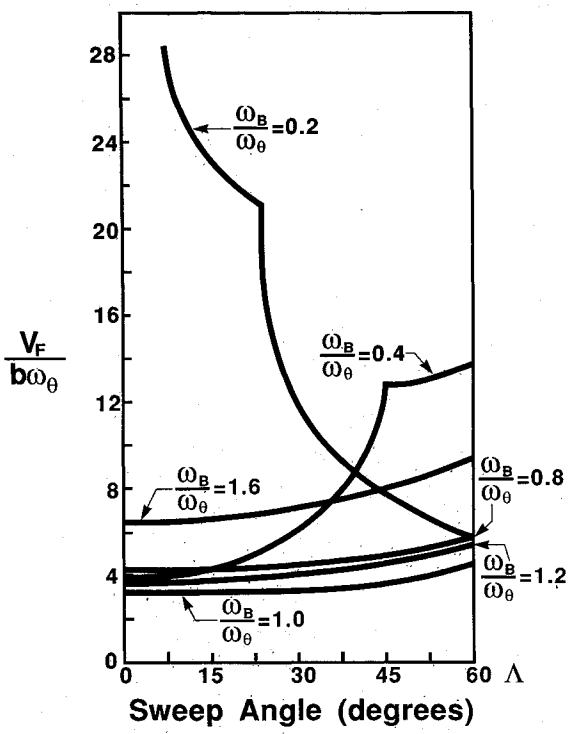

Fig. 8 Effect of the bending-torsion stiffness parameter ω_B/ω_θ on oblique wing flutter speed $\bar{V}_F$ at different sweep angles and $M=2.5$.

predicted by supersonic theory to also lie at the midchord. The effect of the colinearity between the shear centers and the aerodynamic centers is seen from the curve labeled RA = 0 in Fig. 6. Because neither elastic coupling nor aerodynamic coupling is present, divergence is not possible at zero sweep. Bending divergence is possible only if Λ is nonzero and the wing lies in the forward-swept region.

Moving the RA forward of the wing midchord ($a<0$) creates favorable aerodynamic coupling, which creates washout by twisting the wing down when the wing develops increased loads due to bending. As a result, the wing tends to unload itself somewhat, as evidenced by the rightward shift in the stability curves shown in Fig. 6. A combination of negative cross-coupling (bend-up/twist-down) due to forward ply orientation and a forward position of the reference axis should create large divergence speeds.

Introduction of stiffness cross-coupling, or Ψ, into the design creates elastic coupling along the reference axis. The aeroelastic effect of this elastic coupling is equivalent to the geometrical coupling effects of planform sweep. Reference 12 defines a parameter that is used to categorize subcritical wing static aeroelastic behavior. In terms of the parameters used for this study, the "sweep" parameter P is defined as

$$P=\frac{L}{ba}\left[\frac{\tan\Lambda-\Psi/\sqrt{R}}{1-\Psi\sqrt{R}\tan\Lambda}\right]R \qquad (23)$$

Equation (23) contains the parameter R, defined as $R=GJ/EI$, rather than the ratio ω_B/ω_θ used for the present study.

When the structure is orthotropic, with the reference axis position a and primary stiffness ratio R fixed, the sweep parameter is a function only of geometric sweep Λ. With stiffness cross-coupling included, the sweep angle and Ψ appear together so that the parameter $\Psi/\sqrt{R}$ may be thought of as an effective aeroelastic sweep (the analogy is not perfect, since Ψ also appears in the denominator). When the wing is swept forward [$\Lambda<0$ in Eq. (23)], the deliterious effects of forward sweep can be canceled by adding negative Ψ to the design to keep P close to zero, as has been illustrated in Fig. 5. When used on both oblique wing halves, the effect of Ψ is to aeroelastically unsweep the wing, as illustrated in the next section.

Effect of Wing/Fuselage Roll Freedom on Aeroelastic Stability

The results in the previous section agree qualitatively with previously published studies on divergence tailoring. With roll excluded, we had effectively assumed that the roll inertia of the fuselage, defined as I_f in Eq. (12), is infinite or that the ratio I_0/I_f is zero. As a result, motion of the two wing portions of the oblique wing was decoupled. When the aircraft wing-body combination is allowed to roll in response to a small initial disturbance, the dynamic eigenvalue problem must be considered. In this case, the eigenvalue becomes $s=\sigma/\omega_\theta+j\omega/\omega_\theta$ and λ^2 resumes its role as a system parameter.

If the ratio I_0/I_f is not zero, the possibility exists that inertia coupling can alter the aeroelastic stability significantly. Consider Fig. 7, which shows the results of a roll-free stability (flutter) analysis at fixed Mach number ($M=2.5$). This example has no stiffness cross-coupling, i.e., $\Psi=0$. Three different values of the ratio I_0/I_f were considered.

One portion of the flutter stability boundary closely resembles the divergence boundaries seen in previous figures, but displaced slightly to the right, indicating that the presence of roll freedom is stabilizing. This stability boundary, associated with larger oblique wing sweep angles, say above 20 deg, is associated with relatively low reduced frequencies [defined as $\omega b/V$ or $(\omega/\omega_\theta)/\bar{V}$]. The instability in this region is "bending driven," meaning that the streamwise angle of attack generated by bending displacement generates significant aerodynamic forces that tend to predominate over those due to torsion. An examination of the eigenvector associated with this instability shows that both wings deflect upward, in phase, to create an unbalanced roll moment. As the wings flex downward, the roll moment reverses, setting up an oscillatory rocking motion about the fuselage centerline. This instability has been observed in *ad hoc* wind-tunnel tests.

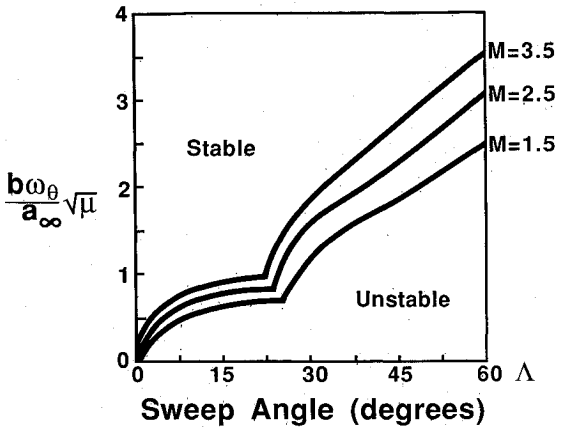

Fig. 9 Altitude-stiffness parameter β vs oblique wing sweep angle for three Mach numbers. Regions above each boundary are stable regions.

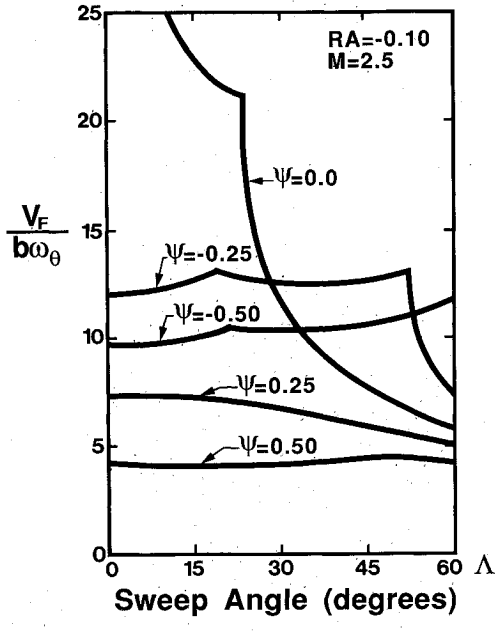

Fig. 10 Effect of stiffness cross-coupling on roll-free oblique wing aeroelastic stability. Symmetrical spanwise ply structural arrangement is used, $M=2.5$.

At lower sweep angles, the flutter instabilities are associated with more classical bending-torsion flutter that have higher reduced frequencies, but have very little fuselage rolling motion apparent. Note that the curve labeled $I_0/I_f=10$ in Fig. 7 has three distinct segments, indicating sweep-angle-dependent switching between critical modes.

Figure 8 shows the effects on flutter of changing the wing bending-torsion frequency ratio for a wing with roll freedom and $I_0/I_f=5$, but with Ψ still zero. It is seen from Fig. 8 that, unless the uncoupled bending frequency is rather low in comparison to the uncoupled torsion frequency, unfavorable stability behavior can result when ω_B/ω_θ is increased, particularly at low sweep angles. If we regard ω_θ as fixed and then change ω_B to effect changes in the ratio ω_B/ω_θ, we see that the "bending-driven" low-frequency flutter boundary moves to the right (and perhaps upward) as expected. On the other hand, values of the frequency ratio ω_B/ω_0 closer to unity have a deliterious effect on flutter similar to that observed on conventional symmetrical aircraft.

Figure 8 also indicates that careful consideration must be given to the choice of ω_B/ω_θ in any demonstrative parameter study. It can be shown that, in terms of the parameters and assumed modes used in the present study, the relationship between ω_B/ω_θ and the problem parameters is

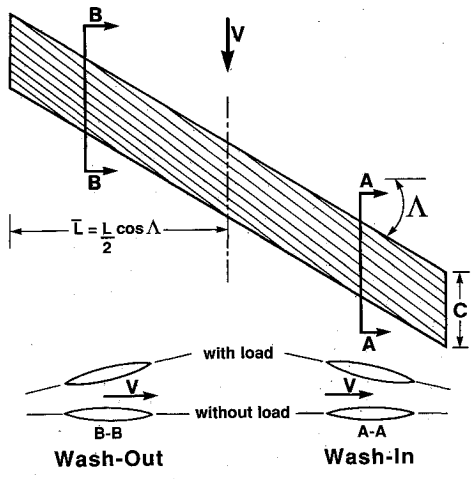

Fig. 11 Asymmetrical ply arrangement for oblique wing stability enhancement.

$$\frac{\omega_B}{\omega_\theta}=0.72\pi\left(\frac{r_\theta}{\bar{R}}\right)\sqrt{\frac{EI}{GJ}} \tag{24}$$

In this case, a value $\omega_B/\omega_\theta=0.20$ is realistic and was used in the rest of the study. Note, however, the wide range of possibilities present in Fig. 8 and the difficulty of making any sweeping conclusions about parametric influence on flutter.

The results presented thus far have been generated at constant Mach number ($M=2.5$) and plotted against oblique wing sweep angle Λ and the parameter $\bar{V}=Vb/\omega_\theta$. To establish the actual flutter velocity, a match point must be determined by first selecting the altitude for which $\mu=50$ and then establishing the speed of sound, a_∞. A horizontal line at $\bar{V}=2.5a_\infty/b\omega_\theta$ must then be drawn on Fig. 8 to locate the critical sweep angle at this altitude, Mach number combination.

An alternative data presentation is shown in Fig. 9 and plots the altitude-stiffness parameter β against sweep angle. The altitude stiffness parameter [previously defined as $\beta=(b\omega_\theta/a_\infty)\sqrt{\mu}$] makes it possible to survey critical combinations of altitude (a_∞ and $\sqrt{\mu}$) and stiffness (ω_θ) at different sweep angles. Figure 9 is unusual in that the region above the boundary is the stable region. The destabilizing effect of oblique wing sweep and increasing Mach number is apparent.

Effect on Flutter of the Stiffness Cross-Coupling Parameter Ψ

We now come to the main purpose of this paper, the examination of the effect of the nondimensional parameter Ψ on supersonic oblique wing flutter. Two basic types of structural configurations are considered. The first type of configuration incorporates a spanwise-symmetrical, advanced composite ply orientation; the second type uses an antisymmetrical configuration. We will consider the spanwise-symmetric structure first.

Spanwise ply symmetry (as opposed to cross-sectional symmetry) means that the parameter Ψ is the same for both wings, i.e., if one wing tends to washout due to elastic coupling so, too, does the other. This can happen only if the plies that furnish the cross-coupling effect are discontinuous at the fuselage intersection and have a V-shape when viewed from above.

Figure 10 shows the results of a flutter analysis in which the critical reduced airspeed parameter $\bar{V}=Vb/\omega_\theta$ is plotted against oblique wing sweep angle, Λ, for the spanwise-symmetrical configuration. The effects of five different values of Ψ (including $\Psi=0$) are shown in Fig. 10.

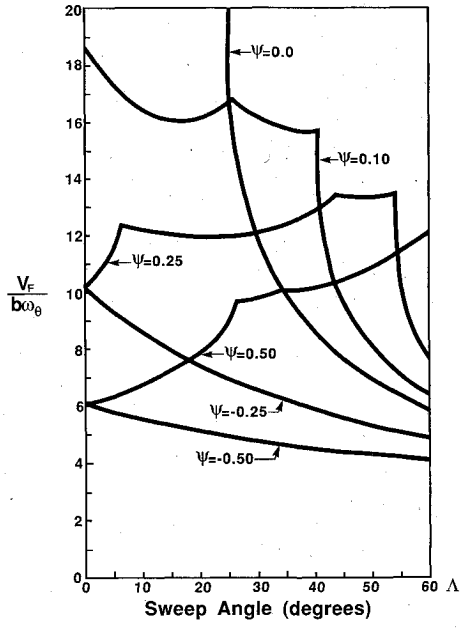

Fig. 12 Effect of asymmetrical stiffness cross-coupling on roll-free oblique wing aeroelastic stability. $M=2.5$; $I_0/I_f=5$. Values of Ψ shown on the figure are those for the aft-swept wing.

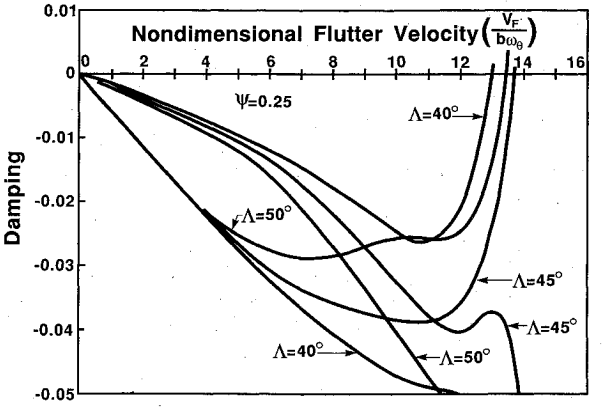

Fig. 13 Damping (σ/ω_θ) as a function of nondimensional velocity at three different oblique wing sweep angles, illustrating mode switching. Asymmetrical ply orientation with $\psi=0.25$ on the aft-swept wing.

The addition of wing elastic washout ($\Psi<0$) causes the low-frequency, body-freedom flutter boundary to move to the right, as one would expect. However, the higher-frequency bending-torsion flutter boundary is displaced downward when washout is added. This downward movement occurs because, for root-fixed symmetrical wings, improvements in the divergence speed through washout cross-coupling are achieved at the expense of lowering the flutter speed. These tendencies are seen to carry over to the oblique wing configuration. Instances of critical mode switching are also apparent in Fig. 10, indicating that complex modal coupling is created by the addition of stiffness cross-coupling.

When a spanwise-symmetrical wash-in laminate is created (Ψ greater than zero), both the aft-swept and forward-swept wings are aeroelastically destiffened by wash-in. The result is the effect observed on the two lower curves ($\Psi=0.25$ and 0.50) in Fig. 10, where it is seen that the body-freedom mode is destabilized.

From a theoretical point of view (and perhaps a manufacturing viewpoint), it would be more sensible to design aeroelastic washout into the forward-swept wing and wash-in into the aft-swept wing. Such a procedure would improve the stability characteristics of the forward-swept wing as well as the lift effectiveness of the aft-swept wing. As indicated by Eq. (23), the addition of $-\Psi$ to a forward-swept wing ($\Lambda<0$) and $+\Psi$ to the aft-swept wing ($\Lambda>0$) will aeroelastically "desweep" the oblique wing angle, while still preserving the advantages of aerodynamic sweep. This unsymmetrical configuration, constructed by laying continuous plies across the wing, is shown in Fig. 11.

Figure 12 shows the results of stability calculations for a roll-free oblique wing with different amounts of asymmetrical stiffness cross-coupling. Trends similar to those observed previously when symmetrical stiffness cross-coupling was employed are seen, with the exception that the high-frequency bending-torsion flutter boundary is not as unfavorably affected by the introduction of asymmetrical stiffness cross-coupling. Note that the Ψ values labeled on this figure are those present of the aft-swept portion.

Some of the complexities introduced by asymmetrical stiffness cross-coupling and asymmetrical sweep are clearly evident in the stability boundaries shown in Fig. 12. When Ψ is 0.25 on the aft wing (and -0.25 on the forward wing) there is evidence of switching between critical modes when the oblique wing sweep angle is in the vicinity of $\Lambda=8$, 45, and 55 deg. Consider the flutter behavior when the sweep angle Λ is near 45 deg.

Changing the oblique wing sweep angle can trigger a mode switch, as can be seen in Fig. 13. In this figure, the value of the damping parameter σ/ω_θ (the real part of the eigenvalue s) is plotted against $\bar{V}=V/b\omega_\theta$ for two distinct vibration modes, at three different sweep angles, while Ψ is held fixed. When $\Lambda=40$ deg, a body-freedom mode with wing bending and significant roll motion coupling is critical. When wing sweep is increased, the crossing point for flutter in this mode, $\sigma/\omega_\theta=0$, moves outward until, at $\Lambda=45$ deg, it no longer crosses the axis. However, there is a simultaneous change in damping in a second bending-torsion mode that causes it to become critical; its crossing point moves to the left as Λ is increased from $\Lambda=40$ to 50 deg and, as a result, only a small change in $\bar{V}_F$ is recorded as the sweep angle increases. The result is that this mode becomes critical near $\Lambda=45$ deg, indicative of the complexities of the oblique wing flutter phenomenon.

Summary and Conclusions

The development of a theoretical model of an aeroelastic oblique wing that is economical, but still relevant, has been described. This model has been used in a number of flutter and divergence studies to illustrate the complex interactions among diverse parameters such as wing bending-torsion stiffness, sweep angle, and stiffness cross-coupling. These results indicate that lessons learned and opportunities available in the aeroelastic tailoring of symmetrical aircraft can be carried over to oblique wing design.

The freedom of the oblique wing/fuselage combination to roll as the result of an aeroelastic disturbance tends to stabilize the aircraft at moderate to large sweep angles (as compared to the stability of a similar wing whose root is held fixed). At lower sweep angles, instability occurs as the result of classical bend-twist wing flutter with a minimal amount of roll motion influence. The introduction of bend-twist stiffness cross-coupling to stabilize the wing/fuselage body-freedom flutter mode, which is bending stiffness critical, tends to destabilize the classical bending-torsion flutter mode. As a result, the inclusion of excessive amounts of cross-coupling may be counterproductive, depending on the oblique sweep angle at which the aircraft is operating.

The addition of stiffness cross-coupling into a design can increase the complexity of the dynamic interactions between modes of motion to the extent that some modes of stability switch from being critical to being noncritical. When stiffness cross-coupling is added to the configuration in a spanwise antisymmetrical manner, the result is an effective static aeroelastic desweeping of the wing that may possibly enhance

stability while preserving the advantages of aerodynamic sweep. The result is that aeroelastic tailoring, when done correctly, may provide additional increased aeroelastic performance while preserving the fundamental advantages of oblique wing sweep at high speeds.

Acknowledgments

This research was sponsored by the Naval Air Development Center, Warminster, PA, under Contract N62269-85-C-0268. Mr. Robert Richey was the Technical Monitor.

References

[1]Gregory, T. A., "Oblique Wing Ready for Research Aircraft," *Aerospace America,* Vol. 23, June 1985, pp. 78–83.

[2]Weisshaar, T. A. and Ashley, H., "Static Aeroelasticity and the Flying Wing," *Journal of Aircraft,* Vol. 10, Oct. 1973, pp. 586–594.

[3]Weisshaar, T. A. and Ashley, H., "Static Aeroelasticity and the Flying Wing—Revisited," *Journal of Aircraft,* Vol. 11, Nov. 1974, pp. 718–720.

[4]Weisshaar, T. A. and Crittenden, J. B., "Flutter of Asymmetrically Swept Wings," *AIAA Journal,* Vol. 14, Aug. 1976, pp. 993–994.

[5]Jones, R. T. and Nisbet, J. W., "Aeroelastic Stability and Control of an Oblique Wing," *Journal of the Royal Aeronautical Society,* Vol. 80, Aug. 1976, pp. 365–369.

[6]Crittenden, J. B., Weisshaar, T. A., Johnson, E. H., and Rutkowski, M. J., "Aeroelastic Stability Characteristics of an Oblique Winged Aircraft," *Journal of Aircraft,* Vol. 15, July 1978, pp. 429–434.

[7]Weisshaar, T. A. and Foist, B. L., "Vibration Tailoring of Advanced Composite Lifting Surfaces," *Journal of Aircraft,* Vol. 22, Feb. 1985, pp. 141–147.

[8]Oyibo, G. A. and Berman, J. H., "Influence of Warpage on Composite Aeroelastic Theories," AIAA Paper 85-0710, April 1985.

[9]Morgan, H. G., Huckel, V., and Runyan, H. L., "Procedure for Calculating Flutter at High Supersonic Speed Including Camber Deflections, and Comparison with Experimental Results," NACA TN 4335, Sept. 1958.

[10]Van Dyke, M. D., "A Study of Second-Order Supersonic Flow Theory," NACA Rept. 1081, 1952.

[11]Weisshaar, T. A., "Aeroelastic Tailoring of Oblique Wing Aircraft," Final Report, Naval Air Development Center Contract N62269-85-C-0268, Purdue Univ., W. Lafayette, IN, Aug. 1987.

[12]Weisshaar, T. A., "Forward Swept Wing Aeroelasticity," AFFDL-TR-79-3087, Air Force Flight Dynamics Lab., Wright-Patterson AFB, OH, June 1979.

Recommended Reading from the AIAA Progress in Astronautics and Aeronautics Series . . .

Tactical Missile Aerodynamics

Michael J. Hemsch and Jack N. Nielsen, editors

Presents a comprehensive updating of the field for the aerodynamicists and designers who are actually developing future missile systems and conducting research. Part I contains in-depth reviews to introduce the reader to the most important developments of the last two decades in missile aerodynamics. Part II presents comprehensive reviews of predictive methodologies, ranging from semi-empirical engineering tools to finite-difference solvers of partial differential equations. The book concludes with two chapters on methods for computing viscous flows. In-depth discussions treat the state-of-the-art in calculating three-dimensional boundary layers and exhaust plumes.

TO ORDER: Write AIAA Order Department, 370 L'Enfant Promenade, S.W., Washington, DC 20024

Please include postage and handling fee of $4.50 with all orders. California and D.C. residents must add 6% sales tax. All foreign orders must be prepaid. Please allow 4-6 weeks for delivery. Prices are subject to change without notice.

1986 858 pp., illus. Hardback
ISBN 0-930403-13-4
AIAA Members $69.95
Nonmembers $99.95
Order Number V-104